

Need for Speed: Zero-Shot Depth Completion with Single-Step Diffusion

Jakub Gregorek^{1,2} Paraskevas Pegios^{1,2}
Theodora Kontogianni^{1,2}

Nando Metzger³ Konrad Schindler³
Lazaros Nalpantidis^{1,2}

¹DTU - Technical University of Denmark

²Pioneer Centre for AI

³ETH Zürich

Abstract

We introduce *Marigold-SSD*, a single-step, late-fusion depth completion framework that leverages strong diffusion priors while eliminating the costly test-time optimization typically associated with diffusion-based methods. By shifting computational burden from inference to finetuning, our approach enables efficient and robust 3D perception under real-world latency constraints. *Marigold-SSD* achieves significantly faster inference with a training cost of only 4.5 GPU days. We evaluate our method across four indoor and two outdoor benchmarks, demonstrating strong cross-domain generalization and zero-shot performance compared to existing depth completion approaches. Our approach significantly narrows the efficiency gap between diffusion-based and discriminative models. Finally, we challenge common evaluation protocols by analyzing performance under varying input sparsity levels. Page: <https://dtu-pas.github.io/marigold-ssd/>

1. Introduction

Depth completion aims to recover a dense depth map from sparse measurements given an input RGB image and is a core task for applications such as autonomous driving, robotics, and 3D reconstruction [26, 77]. In real-world settings, depth sensors such as LiDAR provide only partial information, while downstream tasks require dense depth maps to reason about scene structure. Despite significant progress, many existing methods rely on discriminative models [13, 49, 61, 69, 87] whose performance often degrades under varying sparsity patterns and domain shifts, limiting their applicability in open-world scenarios. This has motivated growing interest in zero-shot evaluations and approaches [4, 36, 65, 90], where models are expected to generalize without dataset-specific retraining.

Recent work [6, 17, 21, 29, 81] leverages strong visual priors learned by foundation models trained on large-scale data [48, 55]. Among these, generative diffusion-based methods [17, 21, 23, 32], such as *Marigold* [29], which re-

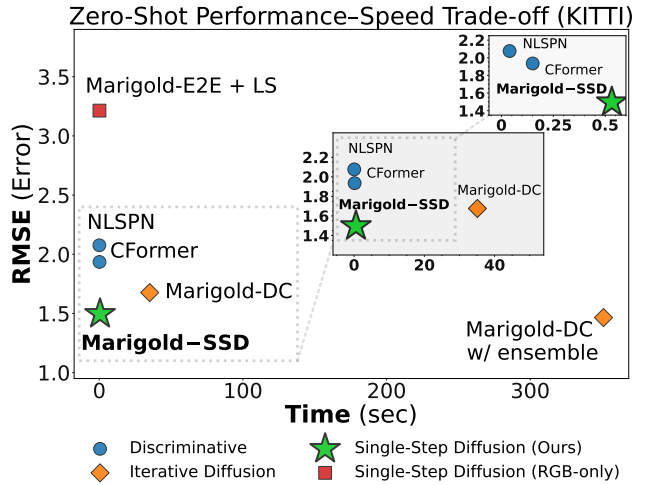


Figure 1. **Performance vs speed trade-off.** Comparison of our method **Marigold-SSD** with other diffusion-based approaches *Marigold-DC* [65] and *Marigold-E2E* [44] + LS (w/o sparse condition) as well as discriminative baselines [49, 87] on KITTI dataset [19]. **Marigold-SSD** occupies a unique region in the trade-off space closing the efficiency gap to discriminative methods while retaining the benefit of the strong diffusion prior.

purposed Stable Diffusion [55] for depth estimation, have proven particularly effective by encoding rich semantic and geometric structure through iterative denoising. Recently, *Marigold* has been extended through test-time optimization to depth completion [65] and depth inpainting [20], consistently outperforming discriminative approaches in zero-shot settings. However, performance comes at a significant computational cost, as inference typically requires tens or hundreds of denoising steps and previous methods often require ensembling strategies [65], making them impractical for real-time embodied AI applications.

In this work, we focus on reducing the computational complexity of diffusion-based methods for zero-shot depth completion. We argue that iterative paradigms are not strictly necessary to achieve high-quality results. Building on top of **Marigold** [29] and its variants [20, 44, 65], we propose zero-shot depth completion with **Single-Step**

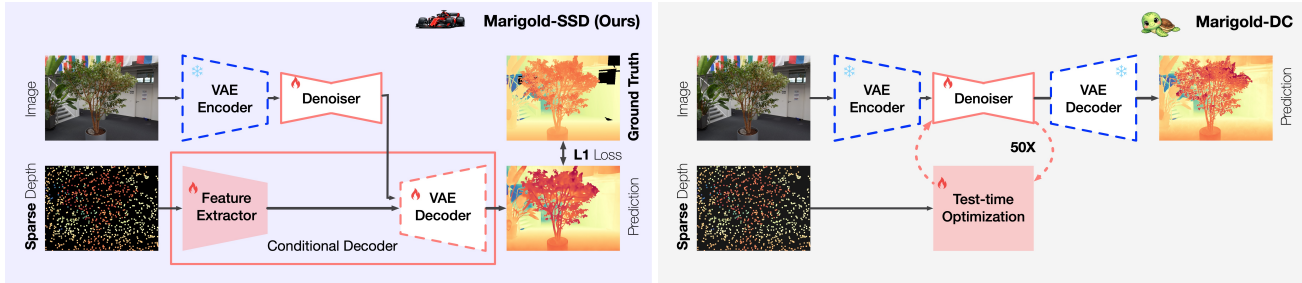


Figure 2. **Marigold-SSD for zero-shot depth completion.** We present a single-step diffusion framework with end-to-end fine-tuning as an efficient alternative to the test-time optimization approach of Marigold-DC [65]. To this end, we introduce a conditional decoder with late fusion to incorporate sparse depth measurements. At inference, our method Marigold-SSD produces high-quality results in a single step, while Marigold-DC typically requires 50 optimization steps per inference and often ensembling 10 inferences for further improvements.

Diffusion (Marigold-SSD), a diffusion-based method that occupies a unique region of the performance-speed trade-off space. As illustrated in Fig. 1, Marigold-SSD achieves performance comparable to state-of-the-art iterative diffusion methods, while being orders of magnitude faster, significantly narrowing the gap between slow but robust diffusion-based approaches and fast discriminative methods.

We demonstrate a single-step diffusion framework for zero-shot depth completion with end-to-end fine-tuning. To enable conditioning on sparse measurements we introduce a late-fusion conditional decoder that injects the condition during decoding. Our design leverages the diffusion prior and enables single-step inference after fine-tuning which takes approximately only 4.5 days on a single NVIDIA H100 GPU. By shifting computation from inference to fine-tuning we provide a practical path towards narrowing the gap between performance and runtime efficiency. A comparison with test-time optimization approaches is shown in Fig. 2. Our method yields strong zero-shot performance across four diverse indoor and two outdoor benchmarks.

Our main contributions are the following:

- The first single-step diffusion-based method for depth completion, significantly faster than diffusion baselines while delivering better performance on average, and remaining competitive even when baselines employ ensembling at substantially higher computational cost.
- A simple yet effective late-fusion strategy for conditioning on sparse measurements, whose effectiveness against early-fusion is validated through ablation studies.
- A comprehensive zero-shot evaluation across indoor and outdoor datasets, demonstrating strong robustness of Marigold-SSD to varying condition sparsity levels, while revealing limitations of existing evaluation benchmarks.

2. Related Work

Zero-Shot Depth Estimation. The zero-shot depth estimation was spearheaded by MiDaS [53], introduc-

ing parametrization and losses allowing mixing training datasets originating from different sources, including 3D movies. The follow up work ZoeDepth [5] innovated on the architecture, and introduced metric bins allowing to estimate metric depth. Piccinelli et al. [51, 52] proposed methods disentangling camera parameters from geometry of the 3D scene exploiting spherical representation. DepthAnything [81] takes advantage of large amount of diverse and unlabeled data. The subsequent work benefited from replacing real data by synthetic and scaling up the teacher model [82]. Another discriminative model, Depth Pro [6], was focusing on boundary accuracy and cross-domain focal-length estimation. Wang et al. [67] takes advantage of geometry supervision techniques, like point cloud alignment solver and multi-scale alignment loss. The work was later extended for metric depth estimation [68]. Majority of the latest models [6, 51, 52, 67, 68, 81, 82] benefit from the ViT architecture initialized from DINOv2 [48]. Even though these models are not grounding their results on real measurements, zero-shot depth estimation models are relevant as strong priors which can be exploited for the task of depth completion.

Depth Completion. Spatial Propagation Networks (SPNs) constitute a widely adopted family of models for depth completion, originally proposed by Liu et al. [40] and subsequently extended to more variants [8, 9, 38, 49]. SPN modules have further been enhanced in numerous follow-up methods [27, 46, 58, 61, 71, 75, 79, 80, 87, 88]. Most depth completion pipelines leverage guidance from a monocular RGB image [60, 66, 70], including the majority of SPN-based approaches. Additional modalities such as surface normals [58] and semantic segmentation [46] have also been explored, alongside completion without explicit guidance [47]. While many methods process sparse depth samples projected onto the image plane, others employ multi-planar projections [79] or operate directly on raw point clouds [76, 83, 88, 89]. Wang et al. [69] demonstrated the advantages of depth pre-completion performed via

Conditional Decoder \mathcal{D}_C

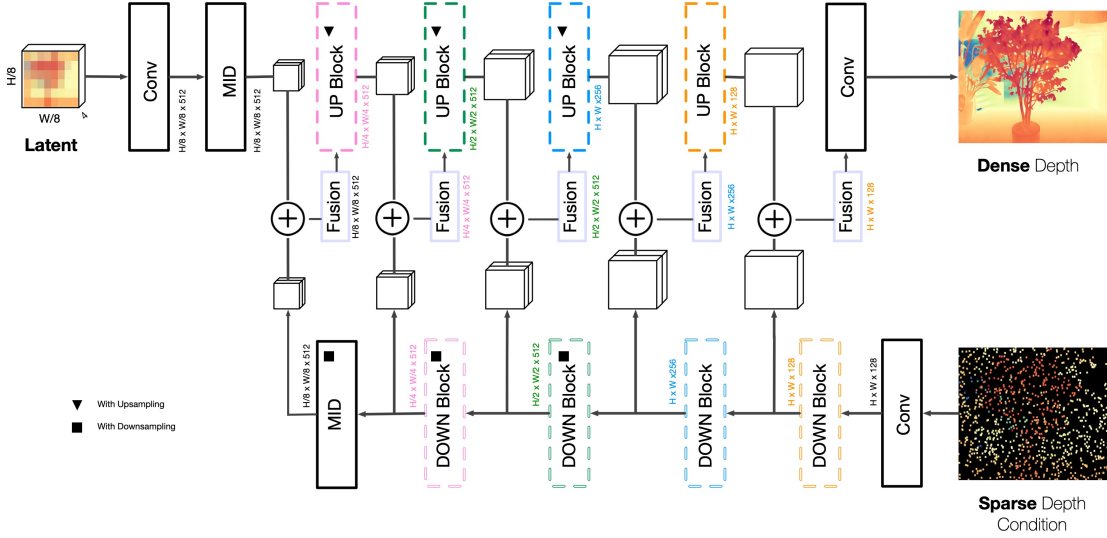


Figure 3. **Internal architecture of the conditional decoder.** \mathcal{D}_C consists of the VAE decoder \mathcal{D} (top row) and blocks processing the sparse condition \mathcal{C} (bottom row), adapted from the VAE encoder \mathcal{E} (differing in down-sampling positions). Feature maps are concatenated channel-wise (\oplus) at five levels and the fusion blocks use 1×1 convolutions (Eq. 1). Conv denotes standard convolution layers, UP, DOWN, and MID blocks are ResNet [24]-based, and MID blocks additionally containing an attention layer.

classical image processing techniques [33]. Several works investigate robustness to varying sparsity levels or sampling patterns [3, 4, 13, 20, 90], and others explicitly address noisy depth measurements [75, 91]. A large portion of prior work focuses on single-dataset training and does not emphasize out-of-domain generalization. For zero-shot scenarios, depth completion can benefit from the strong priors of monocular depth estimators [34, 36, 74, 75] or the generalization ability of stereo matching networks [4]. Approaches vary from direct fine-tuning [36, 74, 75] and distillation [34] to test-time optimization [28].

Diffusion-Based Approaches. Diffusion-based approaches have demonstrated strong performance in zero-shot depth estimation [29, 44, 78, 84], depth completion [65], and inpainting [20]. PrimeDepth [84] leverages Stable Diffusion [55] as a feature extractor, while Ke et al. fine-tunes Stable Diffusion 2 [55] for depth estimation introducing Marigold [29]. Hybrid methods combining diffusion and discriminative models have also been explored [50, 86]. The iterative multi-step nature of diffusion enables plug-and-play conditioning with sparse depth maps [20, 65] for depth completion. However, this iterative process comes with substantial computational cost. A practical path toward broader adoption in resource-constrained scenarios is reducing the number of diffusion steps. Ke et al. [30] address this by distilling Marigold into a Latent Consistency Model [43] for few-step inference. Gui et

al. [21] and Xu et al. [78] re-frame the problem using flow matching [39]. Garcia et al. [44] fine-tunes Marigold for single-step diffusion-based depth estimation, dramatically decreasing inference time. In this work, we bring the single-step inference to depth completion.

3. Method

Given an input RGB image $M \in \mathbb{R}^{H \times W \times 3}$ and a sparse depth condition $C \in \mathbb{R}^{H \times W}$, our goal is to predict a dense depth map $D \in \mathbb{R}^{H \times W}$. Our method builds on the generative prior of Marigold [29], adopts a single-step diffusion formulation [44], and extends it to depth completion by incorporating sparse measurements through a late-fusion strategy and an end-to-end fine-tuning scheme.

3.1. Marigold for Diffusion-based Depth Estimation

Marigold [29] formulates monocular depth estimation as an conditional diffusion process [25] in the latent space of a frozen VAE [64] with encoder \mathcal{E} and decoder \mathcal{D} . The forward process corrupts the clean depth latent $x_0 = \mathcal{E}(D)$ by adding Gaussian noise $\epsilon \sim \mathcal{N}(0, I)$ under a variance schedule $\{\beta_t\}_{t=1}^T$, where D is normalized within $[-1, 1]$ and replicated to three channels to match the VAE input. For a timestep $t \in \{1, \dots, T\}$, the noisy latent is $x_t = \sqrt{\alpha_t}x_0 + \sqrt{1 - \alpha_t}\epsilon$, where $\alpha_t = 1 - \beta_t$ and $\bar{\alpha}_t = \prod_{s=1}^t \alpha_s$. Following Stable Diffusion [55], Marigold adopts the v -parameterization [57] and is trained with a mean-squared

error objective. In particular, a UNet [56] denoiser is conditioned on the timestep t , the noisy latent x_t , and the RGB input encoded into the same latent space as $m = \mathcal{E}(M)$, i.e., $\hat{v}_t = v_\theta(x_t \oplus m, t)$, where \oplus denotes channel-wise concatenation, and it is trained to regress the target velocity $v_t^* = \sqrt{\bar{\alpha}_t}\epsilon - \sqrt{1 - \bar{\alpha}_t}x_0$. At inference, Marigold starts from a Gaussian latent $x_T \sim \mathcal{N}(0, I)$ and iteratively applies DDIM [59] sampler for 50 denoising steps. The final latent is decoded to obtain the dense depth prediction, $\hat{D} = \mathcal{D}(\hat{x}_0)$. In practice, Marigold uses test-time ensembling by running inference multiple times, aligning each output with a per-prediction scale and shift, and taking the pixel-wise median of the aligned predictions [29].

3.2. Depth Completion with Single-Step Diffusion

Previous methods such as Marigold-DC [65] leverage Marigold as a strong prior and employ a guided diffusion [10, 15, 72] variant that uses sparse conditions for test-time optimization of the depth latent during denoising. Although this achieves strong zero-shot performance, it is expensive, typically requiring 50 steps per inference and ensembling 10 inferences to improve results. In contrast, as shown in Fig. 2, we shift computation to fine-tuning, enabling single-step inference.

Garcia et al. [44] observed that the previously poor single-step behavior of Marigold [29] largely stemmed from an inference scheduler issue that paired timesteps with inconsistent noise levels. Correcting this with a trailing setting [37] restored more reliable single-step approximations, which can then be distilled through end-to-end fine-tuning. Thus, we fix the timestep to $t = T$ and set noise to zero. Since $\bar{\alpha}_T \approx 0$, the input x_T contains almost no signal from x_0 and we can effectively tune for single-step prediction. Given $m = \mathcal{E}(M)$, the output of the denoiser is used to get the clean latent as $\hat{x}_0 = \sqrt{\bar{\alpha}_T}x_T - \sqrt{1 - \bar{\alpha}_T}\hat{v}_T$. To adapt the architecture for depth completion: (i) we introduce a conditional decoder $\mathcal{D}_{C,\phi}(\cdot)$ to replace the original VAE decoder and inject sparse measurements C , and (ii) we fine-tune the resulting model with a task-specific loss.

Late Fusion with Conditional Decoder. The architecture is illustrated in Fig. 3. The conditional decoder takes the predicted depth latent \hat{x}_0 and the sparse depth condition C , normalized to the same $[-1, 1]$ range as D , and estimates a dense depth map \hat{D} . To inject C in a late-fusion manner, we mirror the multi-scale structure of the original frozen VAE (\mathcal{E}, \mathcal{D}). We introduce a trainable condition feature extractor \mathcal{F} that processes C and extracts $L=5$ multi-scale feature maps $\{f_l^{\mathcal{F}}\}_{l=1}^L$ that match the spatial resolutions of the decoder features $\{f_l^{\mathcal{D}^c}\}_{l=1}^L$ computed from \hat{x}_0 . At each level l , the high-level sparse conditioning features are fused to together with the dense depth features via convolution layers:

$$f_l = \text{CONV}(f_l^{\mathcal{D}^c} \oplus f_l^{\mathcal{F}}), \quad (1)$$

where CONV is a 1×1 convolution. We initialize the decoder from the original frozen VAE decoder \mathcal{D} , while the feature extractor is initialized from \mathcal{E} . Inspired by ControlNet [85], we initialize CONV as a zero convolution layers. This makes the conditioning path output zero at initialization and preserves the behavior of the original VAE decoder. When fine-tuning, the weights gradually increase the contribution of the condition C .

End-to-End Fine-tuning for Depth Completion. We fine-tune our model end-to-end with a task loss rather than the diffusion training objective. Previous works in monocular depth estimation [44] use an affine-invariant loss [53]. Instead, we optimize an L1 loss to match depth prediction \hat{D} with the dense target D encouraging consistency with the conditioning sparse measurements C . During fine-tuning, we uniformly sample the density of the condition in the range $[l\%, h\%]$, where l and h are the lower and upper bounds. We initialize our model from Marigold-E2E [44], keeping the VAE encoder \mathcal{E} fixed and we fine-tune the proposed conditional decoder $\mathcal{D}_{C,\phi}$ together with the denoising UNet, placing stronger emphasis on our decoder to encourage adaptation for depth completion. Our design retains the strong diffusion depth prior while enabling high quality predictions during inference with a single-step.

Single-Step Inference. At test time, we set x_T with zeros for deterministic inference and removing the need for test-time ensembling. Given an RGB input M , we compute $m = \mathcal{E}(M)$ and use the denoiser predict the depth latent \hat{x}_0 . The conditional decoder then combines \hat{x}_0 with the sparse condition C to produce $\hat{D} = \mathcal{D}_{C,\phi}(\hat{x}_0, C)$. Since C and the predicted *relative depth* \hat{D} lie in the VAE range, we recover *metric depth* via a global scale and shift $D^* = a\hat{D} + b$. The parameters (a, b) are obtained by least-squares alignment to *metric sparse measurements* C^* over valid pixels:

$$\arg \min_{a,b} \sum_{i \in \Omega} (a\hat{D}_i + b - C_i^*)^2, \quad (2)$$

where Ω denotes the set of valid sparse depth locations.

4. Experiments and Results

4.1. Datasets and Implementation Details

Training Datasets. Our method has been trained on the Hypersim [54] and Virtual KITTI [7, 18] datasets. Hypersim is a synthetic dataset consisting of 461 indoor scenes; out of which 365 are used in the training, totaling in 54K samples. Samples were downsampled to 640×480 pixels. Virtual KITTI is a synthetic dataset from the autonomous driving domain. All 5 scenes of the dataset were used for training in a variety of weather versions (morning, fog, rain,

Table 1. **Runtime analysis.** Average per-image inference time in **seconds**, throughput in **FPS**, and **relative speedup** compared to Marigold-DC. Runtimes are measured on an NVIDIA RTX 4090 GPU. Resolutions shown next to dataset names denote the input size used for the timing experiment. Marigold-DC is timed **without ensembling** (single run); ensembling (e.g., 10 predictions) would increase runtime approximately linearly.

	Dataset	Marigold-DC		Marigold-SSD (Ours)	
		Time (s)	FPS	Time (s) ($\uparrow \times$)	FPS
INDOOR	ScanNet <small>(640×480)</small>	25.08	0.04	0.38 (66×)	2.6
	IBims-1 <small>(640×480)</small>	24.62	0.04	0.38 (65×)	2.6
	VOID <small>(640×480)</small>	24.98	0.04	0.38 (66×)	2.6
	NYUv2 <small>(640×480)</small>	24.56	0.04	0.38 (65×)	2.6
OUTDOOR	KITTI <small>(1216×352)</small>	35.10	0.03	0.53 (66×)	1.9
	DDAD <small>(768×480)</small>	30.60	0.03	0.45 (68×)	2.2
AVERAGE		27.49	0.04	0.42 (66×)	2.4

sunset, and overcast), which is more than 21K samples. For training, the images were bottom-center cropped to 1216×352 pixels.

Evaluation Datasets. We evaluated the method on four indoor datasets: NYUv2 [45], ScanNet [14], VOID [73], and IBims-1 [31]. NYUv2 and ScanNet were captured with RGB-D sensors, VOID with an active stereo setup, and IBims-1 with a laser scanner. All indoor datasets were processed at 640×480 resolution; NYUv2 results were downsampled and cropped to the standard 304×228 evaluation size. We used 654 images from the NYUv2 test split, 745 images from the ScanNet selected by [65], all 800 VOID images, and all 100 IBims-1 images. We match the depth sampling protocol of [65]. 500 points were sampled for NYUv2 and ScanNet, 1000 for IBims-1, and 1500 points provided by VOID. We also evaluated on two outdoor datasets: KITTI [19, 63] and DDAD [22], both using LiDAR and originating from autonomous driving. For KITTI, we cropped the images to 1216×352 and used the 1000-image validation split. DDAD was processed at 768×480 resolution and completed depth was up-sampled back to full resolution of 1936×1216 for evaluation. We used the official validation set of 3950 images. Following [4, 65], point clouds for both datasets were filtered for outliers [11]. On DDAD, approximately 20% of LiDAR points were sampled for guidance, matching the protocol in [4, 65, 90].

Implementation Details. Our implementation is based on HuggingFace diffusers library [1] initializing weights from [2]. The training strategy follows [44]: mixing HyperSim [54] and Virtual KITTI [7] datasets with 9:1 ratio, training for 20K iterations utilizing AdamW optimizer [42], initial learning rate set to 3×10^{-5} for \mathcal{D}_C and 3×10^{-6}

Table 2. **Speed-performance trade-off.** *Zero-shot* performance on KITTI [19]. All runtimes are evaluated on NVIDIA RTX 4090 GPUs. We time Marigold-SSD and Marigold-DC [65] (Table 1) and VPP4DC [4]. Performance is taken from [65], and runtimes at original resolution for the other discriminative methods from [62].

Type	Method	Time (s) ↓	RMSE ↓
DISCRIMINATIVE	NLSPN [49] (ECCV '20)	0.039	2.076
	BP-Net [61] (CVPR '24)	0.078	-
	CFormer [87] (CVPR '24)	0.151	1.935
	OGNI-DC [90] (ECCV '24)	0.266	-
	VPP4DC [4] (3DV '24)	0.164	1.609
	GBPN [62] (arXiv preprint '26)	0.137	-
DIFFUSION	Marigold-DC [65] (ICCV '25)	35.103	1.676
	Marigold-SSD (Ours)	0.527	1.496

for the UNet, deploying exponential decay after 100-step warm-up, accumulating gradients over 32 steps of size 1. We train two models, sampling the density of depth condition in the ranges $[0.16\%, 5\%]$ and $[0.16\%, 0.5\%]$ (models denoted by \star). The first interval covers densities of all evaluation datasets while the second interval covers density of indoor datasets only. The training was performed on a single NVIDIA H100 GPU requiring only 4.5 days per model.

Evaluation Metrics. Following the common practices for depth completion, we report mean absolute error $MAE = \frac{1}{N} \sum_i |\mathbf{d}_i - \mathbf{g}_i|$, and root mean squared error $RMSE = \sqrt{\frac{1}{N} \sum_i |\mathbf{d}_i - \mathbf{g}_i|^2}$ where \mathbf{d}_i and \mathbf{g}_i denote elements of depth prediction and ground-truth, and $i \in \{1, \dots, N\}$. All reported results are in meters.

4.2. Runtime Analysis

We evaluate the efficiency of our method and report relative speedup over Marigold-DC [65] in Tab. 1. All timings are measured on an NVIDIA RTX 4090 GPU and Marigold-DC is timed without ensembling (single run). Our method achieves an average $66\times$ speedup across indoor and outdoor datasets while also achieving better average performance (Tab. 3). Running the standard 10-sample ensembling strategy in Marigold-DC increases runtime approximately linearly and would result in $660\times$ speedup on average. Furthermore, we analyze the speed-performance tradeoff on KITTI [19] in Tab. 2 and Fig. 1 by comparing diffusion-based and discriminative depth completion methods. Marigold-SSD substantially narrows the efficiency gap to discriminative approaches retaining the benefits of a strong diffusion prior with runtime comparable to the discriminative models.

4.3. Zero-Shot Depth Completion Results

We evaluate our models in zero-shot context and present the results in Tab. 3. We compare with discriminative methods [4, 13, 34, 36, 41, 49, 61, 62, 87, 90] and diffusion-

Table 3. **Comparison to state-of-the-art on six zero-shot benchmarks.** Most values are taken from [65], except for DMD³C [35] and GBPN [62], which are reported from their original papers. Following [65], we omit BP-Net [61] and OGNI-DC [90] on NYUv2 [45] and KITTI [19] and SpAgNet [12] on ScanNet [14] and IBims-1 [31]. Similar to Marigold [29] + optim and Marigold [29] + LS reported in [65], we evaluate Marigold-E2E [44] + LS as a single-step diffusion baseline. Given *the need for speed*, we highlight **best** and **second best** excluding the ensemble approach of Marigold-DC [65] which increases runtime by an order of magnitude. Our model version trained on lower density-levels is denoted by *. The rank expresses an average position of the method in the table per metric and dataset.

Type	Method	Indoor						Outdoor				Average				
		ScanNet		IBims-1		VOID		NYUv2		KITTI		DDAD		MAE↓	RMSE↓	Rank (Count)
DISCRIMINATIVE	NLSPN [49] (ECCV '20)	0.036	0.127	0.049	0.191	0.210	0.668	0.440	0.716	1.335	2.076	2.498	9.231	0.761	2.168	8.50 (12)
	CFormer [87] (CVPR '23)	0.120	0.232	0.058	0.206	0.216	0.726	0.186	0.374	0.952	1.935	2.518	9.471	0.675	2.157	10.00 (12)
	SpAgNet [12] (WACV '23)	–	–	–	–	0.244	0.706	0.158	0.292	0.518	1.788	4.578	13.236	–	–	10.13 (8)
	BP-Net [61] (CVPR '24)	0.122	0.212	0.078	0.289	0.270	0.742	–	–	–	–	2.270	8.344	–	–	11.75 (8)
	VPP4DC [4] (3DV '24)	0.023	0.076	0.062	0.228	0.148	0.543	0.077	0.247	0.413	<u>1.609</u>	1.344	<u>6.781</u>	0.344	<u>1.581</u>	<u>4.00</u> (12)
	OGNI-DC [90] (ECCV '24)	0.029	0.094	0.059	0.186	0.175	0.593	–	–	–	–	<u>1.867</u>	6.876	–	–	4.88 (8)
	DepthLab [41] (arXiv preprint '24)	0.051	0.081	0.098	0.198	0.214	0.602	0.184	0.276	0.921	2.171	4.498	8.379	0.994	1.951	8.58 (12)
	Prompt Depth Anything (CVPR '25)	0.042	0.079	0.088	0.196	0.191	0.605	0.110	0.233	0.934	2.803	2.107	7.494	0.579	1.902	6.83 (12)
	DMD ³ C [35] (CVPR '25)	0.210	0.101	–	–	0.225	0.676	–	–	–	–	2.498	7.766	–	–	10.00 (6)
	GBPN [62] (arXiv preprint '26)	–	–	–	–	0.220	0.680	–	–	–	–	–	–	–	–	12.50 (2)
DIFFUSION	Marigold + optim (CVPR '24)	0.091	0.141	0.167	0.300	0.261	0.652	0.194	0.309	1.765	3.361	22.872	32.661	4.225	6.237	13.25 (12)
	Marigold + LS [29] (CVPR '24)	0.083	0.129	0.154	0.286	0.238	0.628	0.190	0.294	1.709	3.305	8.217	14.728	1.765	3.228	12.08 (12)
	Marigold-E2E + LS [44] (CVPR '25)	0.073	0.116	0.143	0.275	0.233	0.623	0.134	0.224	1.591	3.214	7.901	14.231	1.679	3.114	10.42 (12)
	Marigold-DC ensemble [65]	0.017	0.057	0.045	0.166	0.152	0.551	0.048	0.124	0.434	1.465	2.364	6.449	0.510	1.469	1.75 (12)
	Marigold-DC [65] (ECCV '25)	0.020	<u>0.063</u>	0.062	0.205	<u>0.157</u>	<u>0.557</u>	0.057	0.142	0.558	1.676	2.985	7.905	0.640	1.758	5.08 (12)
	Marigold-SSD * (Ours)	<u>0.022</u>	0.062	<u>0.056</u>	0.182	0.177	0.588	0.045	0.128	2.443	4.070	3.870	7.841	1.102	2.145	5.33 (12)
Marigold-SSD (Ours)	0.027	0.068	0.060	<u>0.185</u>	0.182	0.590	<u>0.052</u>	<u>0.134</u>	<u>0.454</u>	1.496	2.066	6.524	<u>0.474</u>	1.500	3.75 (12)	

based methods [29, 44, 65]. For depth completion methods [29, 44] the sparse depth was used only for aligning shift and scale of the result using: least squares (denoted by LS) or L1 + L2 optimization (denoted by "optim"). We achieve the best average **RMSE of 1.5** and **MAE of 0.474** versus 1.758 and 0.640 respectively for Marigold-DC without ensembling. When ensembling is utilized, Marigold-DC achieves a RMSE of 1.469 and a MAE of 0.510 at the expense of an order of magnitude slower inference. Considering the *need for speed*, we run and compare with Marigold-DC without ensembling in the rest of the paper. Qualitative results on several datasets of Marigold-SSD compared to Marigold-DC can be seen in Fig. 4 & 5.

4.4. Evaluation under Varying Depth Sparsity

We further evaluate our models across a range of sparsity levels, see Fig. 6 & 7. In addition to Marigold-SSD and Marigold-DC, we assess a Barycentric interpolation computed within Delaunay triangulation of the sparse depth condition. The interpolation disregards RGB images and sets depth values outside the convex to zero. Visualizations of the sparse and interpolated depth can be seen in Fig. 8. As expected, performance improves with denser conditioning depth. When the density reaches about 5% (15360 points), even interpolation performs competitively on IBims-1 and NYUv2. On DDAD, as few as 5000 points allow interpolation to outperform more sophisticated models like Marigold-SSD and Marigold-DC. At lower densities (1500 and 500 points), Marigold-SSD outperforms both Marigold-DC and the interpolation method.

4.5. Ablation Study on Fusion Strategies

In this section we challenge our architecture choice of late-fusion by showcasing early-fusion alternatives. We consider two different early-fusion approaches:

- Frozen VAE – Encoding the depth condition by frozen VAE \mathcal{E} and passing it to UNet through extra channels to the UNet (following RGM conditioning of Marigold [29]). During the training only UNet is refined with learning rate 3×10^{-5} .
- Conditional Encoder – An early fusion equivalent of our conditional decoder. Depth condition is encoded by a duplicated branch of VAE \mathcal{E} . The training follows the same protocol as our Marigold-SSD fine-tuning only UNet and conditional encoder.

We evaluate the Frozen VAE in two variants: one conditioned on sparse depth and one on pre-completed depth. Pre-completion is performed using the same barycentric interpolation tested earlier under varying sparsity. Results in Tab. 4 show that all early-fusion models perform on average worse than our late-fusion approach.

5. Discussion

Preserving Diffusion Prior. Our results show that the proposed architecture and training procedure successfully leverage Marigold’s pre-trained knowledge for zero-shot depth completion. On average our method achieves higher score than Marigold-DC improving performance on all datasets with the exception of VOID. Although, employing the ensembling does lead to performance improvement for Marigold-DC, it requires an order of magnitude

Table 4. **Late vs Early Fusion.** Comparison with early-fusion: models with (i) frozen VAE or (ii) a trainable conditional encoder. i.e, an early fusion equivalent of our conditional decoder. Models trained with lower density-level are denoted by \star . The **best** and **second best** results are highlighted for each training setup. Our late fusion strategy outperforms in almost all cases early-fusion approaches.

Method	Condition	ScanNet		IBims-1		VOID		NYUv2		KITTI		DDAD	
		MAE↓	RMSE↓										
Frozen VAE \star	Sparse	<u>0.038</u>	0.075	0.099	0.212	0.254	0.721	0.089	<u>0.173</u>	1.899	3.642	6.590	12.273
Frozen VAE \star	Interpolated	0.022	0.062	<u>0.057</u>	0.178	<u>0.208</u>	0.663	<u>0.064</u>	0.185	0.978	2.418	<u>3.876</u>	<u>9.466</u>
Conditional Encoder \star	Sparse	0.063	0.103	0.131	0.257	0.222	<u>0.615</u>	0.124	0.208	<u>1.521</u>	<u>3.059</u>	7.611	13.747
Marigold-SSD\star	Sparse	0.022	0.062	0.056	<u>0.182</u>	0.177	0.588	0.045	0.128	2.443	4.070	3.870	7.841
Frozen VAE	Sparse	0.045	0.087	0.111	0.237	0.315	0.820	0.105	0.201	1.280	2.860	5.960	11.494
Frozen VAE	Interpolated	0.024	<u>0.070</u>	0.054	0.175	0.224	0.711	<u>0.064</u>	0.220	<u>0.559</u>	<u>1.791</u>	<u>2.209</u>	<u>7.023</u>
Conditional Encoder	Sparse	0.051	0.088	0.112	0.232	<u>0.216</u>	<u>0.619</u>	0.106	<u>0.185</u>	1.372	2.734	6.592	12.123
Marigold-SSD	Sparse	<u>0.027</u>	0.068	<u>0.060</u>	<u>0.185</u>	0.182	0.590	0.052	0.134	0.454	1.496	2.066	6.524

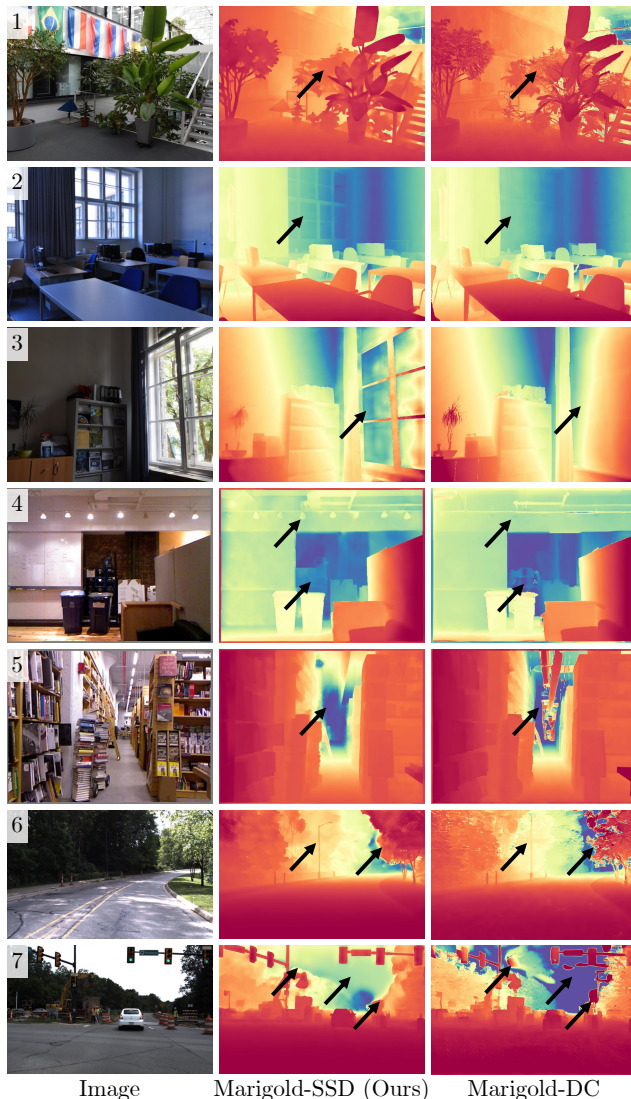


Figure 4. **Qualitative results.** Marigold-SSD generally produces smoother depth maps than Marigold-DC [65], which tends to over-refine details that can lead to unrealistic scene structures.

higher computational budget. Still our method remains competitive while being 660 times faster. Marigold-SSD substantially narrows the efficiency gap to discriminative approaches, retaining the benefits of a strong diffusion prior with near discriminative runtime. Ablations on early-fusion reveal, that the off-the-shelf VAE encoder is ill-suited for sparse depth inputs and refining or rethinking sparse-data fusion is necessary. Pre-completion helps to increase the performance, but the achieved score is still lower compared to our late-fusion approach. Qualitatively, our method produces smoother outputs typical of single-step diffusion, whereas Marigold-DC tends to over-refine details which may lead to unrealistic structures. The differences in perception of details is presented in Fig. 4. We demonstrate that we achieve high quality results in a single step (rows 1 – 3, 6), reducing some of the fine-scale detail over-generation (rows 5, 7).

Limitations. A limitation of our approach is that the sparsity of the depth condition functions as a training hyper-parameter and can influence performance. As demonstrated in our experiments, Marigold-SSD \star trained only on the lower-density corresponding to indoor datasets exhibit a steep drop in accuracy when evaluated on denser outdoor benchmarks. In contrast, Marigold-SSD trained on a broader spectrum of sparsity levels achieves more consistent performance across domains. A potential direction for improvement lies in adaptive normalization strategies scaling the depth condition to the VAE’s operational range. This would mitigate the possible depth inaccuracies, which occur when depth range of the scene deviates from the range of the depth condition. Additionally, developing a training strategy to better model outdoor depth distribution may reduce the characteristic bias of Marigold-based approaches in sky regions (see row 7 of Fig. 4 and Fig. 5).

Performance under variety of sparsity levels. Zero-shot depth completion is inherently challenging. To illustrate when sophisticated models provide real value, we include



Figure 5. **Qualitative results.** Both Marigold-SSD and Marigold-DC tend to underestimate sky depth on KITTI and DDAD, consistent with prior Marigold limitations and limited conditioning information in the sky, while they differ in how they estimate fine scene details.

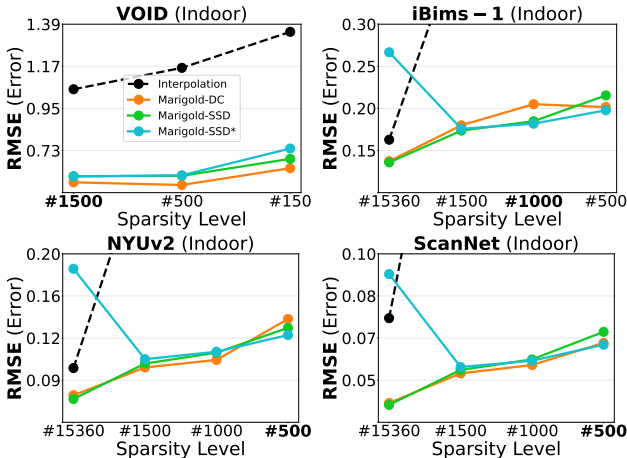


Figure 6. **Evaluation under multiple levels of depth density,** for IBims-1, VOID, NYUv2 and ScanNet datasets. The density of the depth condition is denoted by number of depth samples (#). Only RMSE is presented as the trends for MAE are the same.

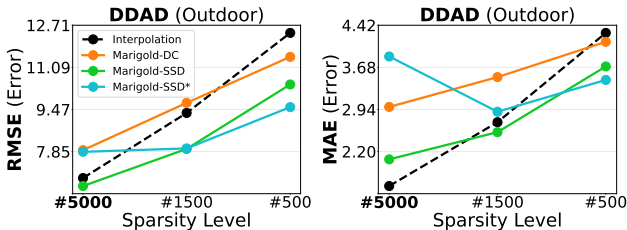


Figure 7. **Challenging the models on DDAD.** At the commonly used sparsity level of 5000 points even sophisticated models can be outperformed by trivial Barycentric interpolation.

a comparison against a simple baseline: barycentric interpolation over a Delaunay triangulation of the sparse depth condition. As expected, increasing the input density raises the chance that simple interpolation approaches achieve performance comparable to state-of-the-art methods. Our analysis shows that the commonly used evaluation density for the DDAD dataset (adapted from [4, 65, 90]) lies well beyond this threshold. The barycentric interpolation (scoring MAE 1.598, RMSE 6.831) surpasses many of evaluated methods under this setting. The models with

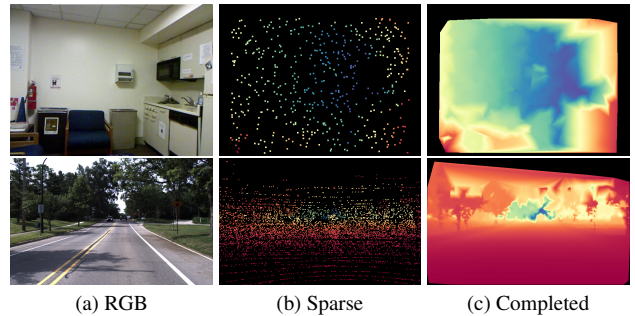


Figure 8. **Barycentric interpolation.** Example of completing sparse depth using Barycentric interpolation within Delaunay triangulation. RGB image is provided here only for reference.

strong pretrained priors can offer their advantages over computationally inexpensive alternatives at lower density levels, i.e. 500 points, similar to established protocols for NYUv2 and ScanNet. At these lower sparsity levels, our method outperforms Marigold-DC.

6. Conclusion

We presented Marigold-SSD, a late-fusion depth-completion framework achieving a 66× speed-up and improved accuracy reaching 1.5 RMSE compared to 1.758 RMSE of Marigold-DC (w/o ensembling). This is achieved while requiring only 4.5 GPU-days for finetuning. We also identified that computationally inexpensive interpolation can achieve competitive zero-shot results on DDAD dataset under standard density levels.

Acknowledgments

This work has been funded by the EU Horizon Europe project “RoBétArmé” under the Grant Agreement 101058731. Part of the work was conducted during a research stay at ETH Zürich. The HPC resources were provided by the Pioneer Centre for Artificial Intelligence in Copenhagen and DTU Computing Center [16].

References

- [1] huggingface/diffusers: State-of-the-art diffusion models for image, video, and audio generation in PyTorch. <https://github.com/huggingface/diffusers>, . [Online; accessed 28-October-2025]. 5
- [2] Hugging Face: GonzaloMG/marigold-e2e-ft-depth. <https://huggingface.co/GonzaloMG/marigold-e2e-ft-depth>, . [Online; accessed 28-October-2025]. 5
- [3] Dimitrios Arapis, Milad Jami, and Lazaros Nalpantidis. Bridging Depth Estimation and Completion for Mobile Robots Reliable 3D Perception. In *Robot Intelligence Technology and Applications 7*, pages 169–179, Cham, 2023. Springer International Publishing. 3
- [4] Luca Bartolomei, Matteo Poggi, Andrea Conti, Fabio Tosi, and Stefano Mattoccia. Revisiting Depth Completion from a Stereo Matching Perspective for Cross-domain Generalization. In *2024 International Conference on 3D Vision (3DV)*, pages 1360–1370, 2024. ISSN: 2475-7888. 1, 3, 5, 6, 8
- [5] Shariq Farooq Bhat, Reiner Birkel, Diana Wofk, Peter Wonka, and Matthias Müller. ZoeDepth: Zero-shot Transfer by Combining Relative and Metric Depth, 2023. 2
- [6] Aleksei Bochkovskii, Amaël Delaunoy, Hugo Germain, Marcel Santos, Yichao Zhou, Stephan R Richter, and Vladlen Koltun. Depth Pro: Sharp Monocular Metric Depth in Less Than a Second. *arXiv preprint arXiv:2410.02073*, 2024. 1, 2
- [7] Yohann Cabon, Naila Murray, and Martin Humenberger. Virtual KITTI 2. *CoRR*, abs/2001.10773, 2020. 4, 5
- [8] Xinjing Cheng, Peng Wang, and Ruigang Yang. Depth Estimation via Affinity Learned with Convolutional Spatial Propagation Network. pages 103–119, 2018. 2
- [9] Xinjing Cheng, Peng Wang, Chenye Guan, and Ruigang Yang. CSPN++: Learning Context and Resource Aware Convolutional Spatial Propagation Networks for Depth Completion. *Proceedings of the AAAI Conference on Artificial Intelligence*, 34(07):10615–10622, 2020. Number: 07. 2
- [10] Hyungjin Chung, Jeongsol Kim, Michael Thompson McCann, Marc Louis Klasky, and Jong Chul Ye. Diffusion posterior sampling for general noisy inverse problems. In *The Eleventh International Conference on Learning Representations*, 2023. 4
- [11] Andrea Conti, Matteo Poggi, Filippo Aleotti, and Stefano Mattoccia. Unsupervised confidence for LiDAR depth maps and applications. In *2022 IEEE/RSJ International Conference on Intelligent Robots and Systems (IROS)*, pages 8352–8359, 2022. 5
- [12] Andrea Conti, Matteo Poggi, and Stefano Mattoccia. Sparsity agnostic depth completion. In *Proceedings of the IEEE/CVF Winter Conference on Applications of Computer Vision*, pages 5871–5880, 2023. 6
- [13] Andrea Conti, Matteo Poggi, and Stefano Mattoccia. Sparsity Agnostic Depth Completion. In *Proceedings of the IEEE/CVF Winter Conference on Applications of Computer Vision (WACV)*, pages 5871–5880, 2023. 1, 3, 5
- [14] Angela Dai, Angel X. Chang, Manolis Savva, Maciej Halber, Thomas Funkhouser, and Matthias Niessner. ScanNet: Richly-Annotated 3D Reconstructions of Indoor Scenes. In *Proceedings of the IEEE Conference on Computer Vision and Pattern Recognition (CVPR)*, 2017. 5, 6
- [15] Prafulla Dhariwal and Alexander Nichol. Diffusion models beat gans on image synthesis. *Advances in neural information processing systems*, 34:8780–8794, 2021. 4
- [16] DTU Computing Center. DTU Computing Center resources. <https://doi.org/10.48714/DTU.HPC.0001>, 2025. 8
- [17] Xiao Fu, Wei Yin, Mu Hu, Kaixuan Wang, Yuexin Ma, Ping Tan, Shaojie Shen, Dahua Lin, and Xiaoxiao Long. Geowizard: Unleashing the Diffusion Priors for 3D Geometry Estimation from a Single Image. In *European Conference on Computer Vision*, pages 241–258. Springer, 2024. 1
- [18] Adrien Gaidon, Qiao Wang, Yohann Cabon, and Eleonora Vig. Virtual Worlds as Proxy for Multi-Object Tracking Analysis. In *Proceedings of the IEEE conference on Computer Vision and Pattern Recognition*, pages 4340–4349, 2016. 4
- [19] Andreas Geiger, Philip Lenz, Christoph Stiller, and Raquel Urtasun. Vision meets Robotics: The KITTI Dataset. *International Journal of Robotics Research (IJRR)*, 2013. 1, 5, 6
- [20] Jakub Gregorek and Lazaros Nalpantidis. SteeredMarigold: Steering Diffusion Towards Depth Completion of Largely Incomplete Depth Maps. In *2025 IEEE International Conference on Robotics and Automation (ICRA)*, pages 13304–13311, 2025. 1, 3
- [21] Ming Gui, Johannes Schusterbauer, Ulrich Prestel, Pingchuan Ma, Dmytro Kotovenko, Olga Grebenkova, Stefan Andreas Baumann, Vincent Tao Hu, and Björn Ommer. DepthFM: Fast Generative Monocular Depth Estimation with Flow Matching. In *Proceedings of the AAAI Conference on Artificial Intelligence*, pages 3203–3211, 2025. 1, 3
- [22] Vitor Guizilini, Rares Ambrus, Sudeep Pillai, Allan Rantotas, and Adrien Gaidon. 3D Packing for Self-Supervised Monocular Depth Estimation. In *IEEE Conference on Computer Vision and Pattern Recognition (CVPR)*, 2020. 5
- [23] Jing He, Haodong Li, Wei Yin, Yixun Liang, Leheng Li, Kaiqiang Zhou, Hongbo Zhang, Bingbing Liu, and Yingcong Chen. Lotus: Diffusion-based visual foundation model for high-quality dense prediction. *arXiv preprint arXiv:2409.18124*, 2024. 1
- [24] Kaiming He, Xiangyu Zhang, Shaoqing Ren, and Jian Sun. Deep Residual Learning for Image Recognition. In *Proceedings of the IEEE Conference on Computer Vision and Pattern Recognition (CVPR)*, 2016. 3
- [25] Jonathan Ho, Ajay Jain, and Pieter Abbeel. Denoising Diffusion Probabilistic Models. In *Advances in Neural Information Processing Systems*, pages 6840–6851. Curran Associates, Inc., 2020. 3
- [26] Junjie Hu, Chenyu Bao, Mete Ozay, Chenyou Fan, Qing Gao, Honghai Liu, and Tin Lun Lam. Deep Depth Completion From Extremely Sparse Data: A Survey. *IEEE Trans-*

- actions on *Pattern Analysis and Machine Intelligence*, 45(7): 8244–8264, 2023. 1
- [27] Mu Hu, Shuling Wang, Bin Li, Shiyu Ning, Li Fan, and Xiaojin Gong. PENet: Towards Precise and Efficient Image Guided Depth Completion. In *2021 IEEE International Conference on Robotics and Automation (ICRA)*, pages 13656–13662, 2021. ISSN: 2577-087X. 2
- [28] Chanhwi Jeong, Inhwan Bae, Jin-Hwi Park, and Hae-Gon Jeon. Test-Time Prompt Tuning for Zero-Shot Depth Completion. In *Proceedings of the IEEE/CVF International Conference on Computer Vision (ICCV)*, pages 9443–9454, 2025. 3
- [29] Bingxin Ke, Anton Obukhov, Shengyu Huang, Nando Metzger, Rodrigo Caye Daudt, and Konrad Schindler. Repurposing Diffusion-Based Image Generators for Monocular Depth Estimation. In *Proceedings of the IEEE/CVF Conference on Computer Vision and Pattern Recognition (CVPR)*, 2024. 1, 3, 4, 6
- [30] Bingxin Ke, Kevin Qu, Tianfu Wang, Nando Metzger, Shengyu Huang, Bo Li, Anton Obukhov, and Konrad Schindler. Marigold: Affordable Adaptation of Diffusion-Based Image Generators for Image Analysis. *IEEE Transactions on Pattern Analysis and Machine Intelligence*, pages 1–18, 2025. 3
- [31] Tobias Koch, Lukas Liebel, Friedrich Fraundorfer, and Marco Korner. Evaluation of CNN-based Single-Image Depth Estimation Methods. In *Proceedings of the European Conference on Computer Vision (ECCV) Workshops*, 2018. 5, 6
- [32] Akshay Krishnan, Xinchun Yan, Vincent Casser, and Abhijit Kundu. Orchid: Image latent diffusion for joint appearance and geometry generation. *arXiv preprint arXiv:2501.13087*, 2025. 1
- [33] Jason Ku, Ali Harakeh, and Steven L. Waslander. In Defense of Classical Image Processing: Fast Depth Completion on the CPU. In *2018 15th Conference on Computer and Robot Vision (CRV)*, pages 16–22, 2018. 3
- [34] Yingping Liang, Yutao Hu, Wenqi Shao, and Ying Fu. Distilling Monocular Foundation Model for Fine-grained Depth Completion. In *Proceedings of the IEEE/CVF Conference on Computer Vision and Pattern Recognition (CVPR)*, pages 22254–22265, 2025. 3, 5
- [35] Yingping Liang, Yutao Hu, Wenqi Shao, and Ying Fu. Distilling monocular foundation model for fine-grained depth completion. In *Proceedings of the Computer Vision and Pattern Recognition Conference*, pages 22254–22265, 2025. 6
- [36] Haotong Lin, Sida Peng, Jingxiao Chen, Songyou Peng, Jiaming Sun, Minghuan Liu, Hujun Bao, Jiashi Feng, Xiaowei Zhou, and Bingyi Kang. Prompting Depth Anything for 4K Resolution Accurate Metric Depth Estimation. In *Proceedings of the IEEE/CVF Conference on Computer Vision and Pattern Recognition (CVPR)*, pages 17070–17080, 2025. 1, 3, 5
- [37] Shanchuan Lin, Bingchen Liu, Jiashi Li, and Xiao Yang. Common diffusion noise schedules and sample steps are flawed. In *Proceedings of the IEEE/CVF winter conference on applications of computer vision*, pages 5404–5411, 2024. 4
- [38] Yuankai Lin, Hua Yang, Tao Cheng, Wending Zhou, and Zhouping Yin. DySPN: Learning Dynamic Affinity for Image-Guided Depth Completion. *IEEE Transactions on Circuits and Systems for Video Technology*, 34(6):4596–4609, 2024. 2
- [39] Yaron Lipman, Ricky T.Q. Chen, Heli Ben-Hamu, Maximilian Nickel, and Matt Le. Flow matching for generative modeling. In *11th International Conference on Learning Representations (ICLR)*, 2023. 3
- [40] Sifei Liu, Shalini De Mello, Jinwei Gu, Guangyu Zhong, Ming-Hsuan Yang, and Jan Kautz. Learning Affinity via Spatial Propagation Networks. In *Advances in Neural Information Processing Systems*. Curran Associates, Inc., 2017. 2
- [41] Zhiheng Liu, Ka Leong Cheng, Qiuyu Wang, Shuzhe Wang, Hao Ouyang, Bin Tan, Kai Zhu, Yujun Shen, Qifeng Chen, and Ping Luo. DepthLab: From Partial to Complete, 2024. 5, 6
- [42] Ilya Loshchilov and Frank Hutter. Decoupled Weight Decay Regularization. In *International Conference on Learning Representations*, 2019. 5
- [43] Simian Luo, Yiqin Tan, Longbo Huang, Jian Li, and Hang Zhao. Latent Consistency Models: Synthesizing High-Resolution Images with Few-Step Inference, 2023. 3
- [44] Gonzalo Martin Garcia, Karim Abou Zeid, Christian Schmidt, Daan de Geus, Alexander Hermans, and Bastian Leibe. Fine-Tuning Image-Conditional Diffusion Models is Easier than You Think. In *Proceedings of the IEEE/CVF Winter Conference on Applications of Computer Vision (WACV)*, 2025. 1, 3, 4, 5, 6
- [45] Pushmeet Kohli Nathan Silberman, Derek Hoiem and Rob Fergus. Indoor Segmentation and Support Inference from RGBD Images. In *ECCV*, 2012. 5, 6
- [46] Danish Nazir, Alain Pagani, Marcus Liwicki, Didier Stricker, and Muhammad Zeshan Afzal. SemAttNet: Toward Attention-Based Semantic Aware Guided Depth Completion. *IEEE Access*, 10:120781–120791, 2022. Conference Name: IEEE Access. 2
- [47] Lucas Nunes, Rodrigo Marcuzzi, Benedikt Mersch, Jens Behley, and Cyrill Stachniss. Scaling Diffusion Models to Real-World 3D LiDAR Scene Completion. In *Proceedings of the IEEE/CVF Conference on Computer Vision and Pattern Recognition (CVPR)*, pages 14770–14780, 2024. 2
- [48] Maxime Oquab, Timothée Darcet, Théo Moutakanni, Huy Vo, Marc Szafraniec, Vasil Khalidov, Pierre Fernandez, Daniel Haziza, Francisco Massa, Alaaeldin El-Nouby, Mahmoud Assran, Nicolas Ballas, Wojciech Galuba, Russell Howes, Po-Yao Huang, Shang-Wen Li, Ishan Misra, Michael Rabbat, Vasu Sharma, Gabriel Synnaeve, Hu Xu, Hervé Jegou, Julien Mairal, Patrick Labatut, Armand Joulin, and Piotr Bojanowski. DINOv2: Learning Robust Visual Features without Supervision, 2024. 1, 2
- [49] Jinsun Park, Kyungdon Joo, Zhe Hu, Chi-Kuei Liu, and In So Kweon. Non-local Spatial Propagation Network for Depth Completion. In *Computer Vision – ECCV 2020*, pages 120–136, Cham, 2020. Springer International Publishing. 1, 2, 5, 6

- [50] Duc-Hai Pham, Tung Do, Phong Nguyen, Binh-Son Hua, Khoi Nguyen, and Rang Nguyen. SharpDepth: Sharpening Metric Depth Predictions Using Diffusion Distillation. In *Proceedings of the IEEE/CVF Conference on Computer Vision and Pattern Recognition (CVPR)*, pages 17060–17069, 2025. 3
- [51] Luigi Piccinelli, Yung-Hsu Yang, Christos Sakaridis, Mattia Segu, Siyuan Li, Luc Van Gool, and Fisher Yu. UniDepth: Universal Monocular Metric Depth Estimation. In *Proceedings of the IEEE/CVF Conference on Computer Vision and Pattern Recognition (CVPR)*, pages 10106–10116, 2024. 2
- [52] Luigi Piccinelli, Christos Sakaridis, Yung-Hsu Yang, Mattia Segu, Siyuan Li, Wim Abbeloos, and Luc Van Gool. UniDepthV2: Universal Monocular Metric Depth Estimation Made Simpler. *IEEE Transactions on Pattern Analysis and Machine Intelligence*, 48(3):2354–2367, 2026. 2
- [53] René Ranftl, Katrin Lasinger, David Hafner, Konrad Schindler, and Vladlen Koltun. Towards Robust Monocular Depth Estimation: Mixing Datasets for Zero-Shot Cross-Dataset Transfer. *IEEE Transactions on Pattern Analysis and Machine Intelligence*, 44(3):1623–1637, 2022. 2, 4
- [54] Mike Roberts, Jason Ramapuram, Anurag Ranjan, Atulit Kumar, Miguel Angel Bautista, Nathan Paczan, Russ Webb, and Joshua M. Susskind. Hypersim: A Photorealistic Synthetic Dataset for Holistic Indoor Scene Understanding. In *International Conference on Computer Vision (ICCV) 2021*, 2021. 4, 5
- [55] Robin Rombach, Andreas Blattmann, Dominik Lorenz, Patrick Esser, and Björn Ommer. High-Resolution Image Synthesis with Latent Diffusion Models. In *Proceedings of the IEEE/CVF Conference on Computer Vision and Pattern Recognition (CVPR)*, pages 10684–10695, 2022. 1, 3
- [56] Olaf Ronneberger, Philipp Fischer, and Thomas Brox. U-net: Convolutional networks for biomedical image segmentation. In *International Conference on Medical image computing and computer-assisted intervention*, pages 234–241. Springer, 2015. 4
- [57] Tim Salimans and Jonathan Ho. Progressive distillation for fast sampling of diffusion models. In *International Conference on Learning Representations*, 2022. 3
- [58] Shuwei Shao, Zhongcai Pei, Weihai Chen, Peter C. Y. Chen, and Zhengguo Li. NDDepth: Normal-Distance Assisted Monocular Depth Estimation and Completion. *IEEE Transactions on Pattern Analysis and Machine Intelligence*, 46(12):8883–8899, 2024. 2
- [59] Jiaming Song, Chenlin Meng, and Stefano Ermon. Denoising diffusion implicit models. In *International Conference on Learning Representations*, 2021. 4
- [60] Jie Tang, Fei-Peng Tian, Wei Feng, Jian Li, and Ping Tan. Learning Guided Convolutional Network for Depth Completion. *IEEE Transactions on Image Processing*, 30:1116–1129, 2021. 2
- [61] Jie Tang, Fei-Peng Tian, Boshi An, Jian Li, and Ping Tan. Bilateral Propagation Network for Depth Completion. In *Proceedings of the IEEE/CVF Conference on Computer Vision and Pattern Recognition (CVPR)*, pages 9763–9772, 2024. 1, 2, 5, 6
- [62] Jie Tang, Pingping Xie, Jian Li, and Ping Tan. Gaussian belief propagation network for depth completion. *arXiv preprint arXiv:2601.21291*, 2026. 5, 6
- [63] Jonas Uhrig, Nick Schneider, Lukas Schneider, Uwe Franke, Thomas Brox, and Andreas Geiger. Sparsity Invariant CNNs. In *International Conference on 3D Vision (3DV)*, 2017. 5
- [64] Aaron Van Den Oord, Oriol Vinyals, et al. Neural discrete representation learning. *Advances in neural information processing systems*, 30, 2017. 3
- [65] Massimiliano Viola, Kevin Qu, Nando Metzger, Bingxin Ke, Alexander Becker, Konrad Schindler, and Anton Obukhov. Marigold-DC: Zero-Shot Monocular Depth Completion with Guided Diffusion, 2024. 1, 2, 3, 4, 5, 6, 7, 8
- [66] Kun Wang, Zhiqiang Yan, Junkai Fan, Jun Li, and Jian Yang. Learning Inverse Laplacian Pyramid for Progressive Depth Completion. *arXiv preprint arXiv:2502.07289*, 2025. 2
- [67] Ruicheng Wang, Sicheng Xu, Cassie Dai, Jianfeng Xiang, Yu Deng, Xin Tong, and Jiaolong Yang. MoGe: Unlocking Accurate Monocular Geometry Estimation for Open-Domain Images with Optimal Training Supervision. In *Proceedings of the IEEE/CVF Conference on Computer Vision and Pattern Recognition (CVPR)*, pages 5261–5271, 2025. 2
- [68] Ruicheng Wang, Sicheng Xu, Yue Dong, Yu Deng, Jianfeng Xiang, Zelong Lv, Guangzhong Sun, Xin Tong, and Jiaolong Yang. MoGe-2: Accurate Monocular Geometry with Metric Scale and Sharp Details, 2025. 2
- [69] Yufei Wang, Bo Li, Ge Zhang, Qi Liu, Tao Gao, and Yuchao Dai. LRRU: Long-short Range Recurrent Updating Networks for Depth Completion. pages 9422–9432, 2023. 1, 2
- [70] Yufei Wang, Yuxin Mao, Qi Liu, and Yuchao Dai. Decomposed Guided Dynamic Filters for Efficient RGB-Guided Depth Completion. *IEEE Transactions on Circuits and Systems for Video Technology*, 34(2):1186–1198, 2024. 2
- [71] Yufei Wang, Ge Zhang, Shaoqian Wang, Bo Li, Qi Liu, Le Hui, and Yuchao Dai. Improving Depth Completion via Depth Feature Upsampling. In *Proceedings of the IEEE/CVF Conference on Computer Vision and Pattern Recognition (CVPR)*, pages 21104–21113, 2024. 2
- [72] Nina Weng, Paraskevas Pegios, Eike Petersen, Aasa Feragen, and Siavash Bigdeli. Fast diffusion-based counterfactuals for shortcut removal and generation. In *European Conference on Computer Vision*, pages 338–357. Springer, 2024. 4
- [73] Alex Wong, Xiaohan Fei, Stephanie Tsuei, and Stefano Soatto. Unsupervised Depth Completion from Visual Inertial Odometry. *IEEE Robotics and Automation Letters*, 5(2): 1899–1906, 2020. 5
- [74] Jijun Xiang, Longliang Liu, Xuan Zhu, Xianqi Wang, Min Lin, and Xin Yang. DEPTHOR++: Robust Depth Enhancement from a Real-World Lightweight dToF and RGB Guidance, 2025. 3
- [75] Jijun Xiang, Xuan Zhu, Xianqi Wang, Yu Wang, Hong Zhang, Fei Guo, and Xin Yang. DEPTHOR: Depth Enhancement from a Practical Light-Weight dToF Sensor and RGB Image. *arXiv preprint arXiv:2504.01596*, 2025. 2, 3
- [76] Rui Xiang, Feng Zheng, Huapeng Su, and Zhe Zhang. 3dDepthNet: Point Cloud Guided Depth Completion Net-

- work for Sparse Depth and Single Color Image. *CoRR*, abs/2003.09175, 2020. [2](#)
- [77] Zexiao Xie, Xiaoxuan Yu, Xiang Gao, Kunqian Li, and Shuhan Shen. Recent Advances in Conventional and Deep Learning-Based Depth Completion: A Survey. *IEEE Transactions on Neural Networks and Learning Systems*, 35(3): 3395–3415, 2024. [1](#)
- [78] Gangwei Xu, Haotong Lin, Hongcheng Luo, Xianqi Wang, Jingfeng Yao, Lianghui Zhu, Yuechuan Pu, Cheng Chi, Haiyang Sun, Bing Wang, Guang Chen, Hangjun Ye, Sida Peng, and Xin Yang. Pixel-perfect depth with semantics-prompted diffusion transformers, 2025. [3](#)
- [79] Zhiqiang Yan, Yuankai Lin, Kun Wang, Yupeng Zheng, Yufei Wang, Zhenyu Zhang, Jun Li, and Jian Yang. Tri-Perspective View Decomposition for Geometry-Aware Depth Completion. pages 4874–4884, 2024. [2](#)
- [80] Zhiqiang Yan, Xiang Li, Le Hui, Zhenyu Zhang, Jun Li, and Jian Yang. RigNet++: Semantic Assisted Repetitive Image Guided Network for Depth Completion. *International Journal of Computer Vision*, pages 1–23, 2025. [2](#)
- [81] Lihe Yang, Bingyi Kang, Zilong Huang, Xiaogang Xu, Jiashi Feng, and Hengshuang Zhao. Depth Anything: Unleashing the Power of Large-Scale Unlabeled Data. In *Proceedings of the IEEE/CVF Conference on Computer Vision and Pattern Recognition (CVPR)*, pages 10371–10381, 2024. [1](#), [2](#)
- [82] Lihe Yang, Bingyi Kang, Zilong Huang, Zhen Zhao, Xiaogang Xu, Jiashi Feng, and Hengshuang Zhao. Depth Anything V2. In *Advances in Neural Information Processing Systems*, pages 21875–21911. Curran Associates, Inc., 2024. [2](#)
- [83] Zhu Yu, Zehua Sheng, Zili Zhou, Lun Luo, Si-Yuan Cao, Hong Gu, Huaqi Zhang, and Hui-Liang Shen. Aggregating Feature Point Cloud for Depth Completion. In *Proceedings of the IEEE/CVF International Conference on Computer Vision (ICCV)*, pages 8732–8743, 2023. [2](#)
- [84] Denis Zavadski, Damjan Kalšan, and Carsten Rother. PrimeDepth: Efficient Monocular Depth Estimation with a Stable Diffusion Preimage. In *Proceedings of the Asian Conference on Computer Vision (ACCV)*, pages 922–940, 2024. [3](#)
- [85] Lvmin Zhang, Anyi Rao, and Maneesh Agrawala. Adding conditional control to text-to-image diffusion models. In *Proceedings of the IEEE/CVF international conference on computer vision*, pages 3836–3847, 2023. [4](#)
- [86] Xiang Zhang, Bingxin Ke, Hayko Riemenschneider, Nando Metzger, Anton Obukhov, Markus Gross, Konrad Schindler, and Christopher Schroers. BetterDepth: Plug-and-Play Diffusion Refiner for Zero-Shot Monocular Depth Estimation. In *Advances in Neural Information Processing Systems*, pages 108674–108709. Curran Associates, Inc., 2024. [3](#)
- [87] Youmin Zhang, Xianda Guo, Matteo Poggi, Zheng Zhu, Guan Huang, and Stefano Mattoccia. CompletionFormer: Depth Completion with Convolutions and Vision Transformers. In *Proceedings of the IEEE/CVF Conference on Computer Vision and Pattern Recognition (CVPR)*, pages 18527–18536, 2023. [1](#), [2](#), [5](#), [6](#)
- [88] Wending Zhou, Xu Yan, Yinghong Liao, Yuankai Lin, Jin Huang, Gangming Zhao, Shuguang Cui, and Zhen Li. BEV@DC: Bird’s-Eye View Assisted Training for Depth Completion. In *Proceedings of the IEEE/CVF Conference on Computer Vision and Pattern Recognition (CVPR)*, pages 9233–9242, 2023. [2](#)
- [89] Kuang Zhu, Xingli Gan, and Min Sun. GAC-Net: Geometric and Attention-Based Network for Depth Completion. *arXiv preprint arXiv:2501.07988*, 2025. [2](#)
- [90] Yiming Zuo and Jia Deng. OGNI-DC: Robust Depth Completion with Optimization-Guided Neural Iterations. In *Computer Vision – ECCV 2024*, pages 78–95, Cham, 2025. Springer Nature Switzerland. [1](#), [3](#), [5](#), [6](#), [8](#)
- [91] Yiming Zuo, Willow Yang, Zeyu Ma, and Jia Deng. OMNI-DC: Highly Robust Depth Completion with Multiresolution Depth Integration. In *Proceedings of the IEEE/CVF International Conference on Computer Vision (ICCV)*, pages 9287–9297, 2025. [3](#)